PHOTON FLUX DENSITY-DEPENDENT GENE EXPRESSION IN *Synechocystis* sp. PCC 6803 IS REGULATED BY A SMALL, REDOX RESPONSIVE, LuxR-TYPE REGULATOR

Kinu Nakamura[1] and Yukako Hihara

From the Department of Biochemistry and Molecular Biology, Faculty of Science, Saitama University, Saitama 338-8570, Japan

Running Title: redox responsive transcriptional regulator in *Synechocystis*

Address correspondence to: Yukako Hihara, Department of Biochemistry and Molecular Biology, Faculty of Science, Saitama University, 255 Shimo-Okubo, Saitama 338-8570, Japan, Tel. +81-48-858-3396; Fax. +81-48-858-3384; E-Mail: hihara@molbiol.saitama-u.ac.jp

[1]Current Address: Laboratory of Molecular Biology, Institute for Chemical Research, Kyoto University, Uji, Kyoto 611-0011, Japan

The expression of many cyanobacterial genes is regulated by the redox state of the photosynthetic electron transport chain. However, factors involved in this regulation have not been identified. In this study, we demonstrate that a small LuxR-type regulator in *Synechocystis* sp. PCC 6803, PedR (Ssl0564), senses the activity of photosynthetic electron transport to achieve the photon flux density-dependent transcriptional regulation. PedR is constitutively expressed in *Synechocystis* cells and exists as a dimer bridged by intermolecular disulfide bond(s). It activates the expression of *chlL*, *chlN*, *chlB* and slr1957 and represses that of *ndhD2*, *rpe* and the *pedR* (ssl0564)-sll0296 operon under the conditions where the activity of photosynthetic electron transport is low. When the supply of reducing equivalents from photosynthetic electron transport chain increases upon the elevation of photon flux density, PedR is inactivated through its conformational change within 5 minutes. This mechanism enables transient induction or repression of the target genes in response to sudden changes in light environment. The fact that orthologs of PedR are conserved among all the cyanobacterial genomes sequenced so far indicates that this type of transcriptional regulation is essential for cyanobacteria to acclimate to changing environments.

Following changes in the environmental conditions such as photon flux density, temperature or nutrient availability, photosynthetic organisms must balance energy supply through photosynthetic electron transport and its consumption by energy-demanding metabolic processes (1). For example, shift from low- to high-light conditions triggers decrease in the amount of the light-harvesting complexes and photosystem reaction centers to down-regulate the energy supply, whereas up-regulation of energy consumption is achieved by activation of metabolic pathways such as CO_2 fixation (2, 3, 4). This coordination is important not only to maximize the efficiency of photosynthesis but also to minimize the damage due to the over-reduction of the photosynthetic electron transport chain that may result in the formation of harmful reactive oxygen species (5).

Recent DNA microarray studies on high-light acclimation of the cyanobacterium *Synechocystis* sp. PCC 6803 revealed the intimate relationship between these acclimation responses and transcriptional regulation (6, 7, 8). Transcript levels of more than 100 ORFs including those involved in light absorption, photochemical reaction, protection from photoinhibition and protein synthesis were strongly affected by the changes in photon flux density. Interestingly, many of these ORFs were shown to be responsive to other environmental stresses such as low temperature (9), high salt (10), low CO_2 (11), hydrogen peroxide (12) and iron deficiency (13). These observations imply that transcription of high-light responsive genes is not regulated by sensing photon flux density *per se*, but by monitoring the intracellular redox levels. It has been proposed that the redox state of the plastoquinone pool is important for

transcriptional regulation of photosynthesis-related genes (14, 15). However, DNA microarray analysis using inhibitors of the photosynthetic electron transport revealed that the redox state of components located downstream of the plastoquinone pool would be more critical for transcriptional regulation than that of the plastoquinone in *Synechocystis* sp. PCC 6803 (16). Similarly, it has recently been shown by DNA microarray technique that the redox state of the components on the acceptor side of photosystem I is important for light-dependent modulation of nuclear gene expression in higher plants (17). These results seem quite reasonable considering that the redox state of the downstream region of photosynthetic electron transport chain can be directly affected by the energy balance of cells. However, actual mechanisms of redox sensing and subsequent processes of signal transduction are totally unknown.

In this study, we report that PedR (Ssl0564) from *Synechocystis* sp. PCC 6803, a small LuxR-type transcriptional regulator, works as a sensor for the availability of reducing equivalents supplied from photosynthetic electron transport chain. Thus, PedR establishes an important link between perception of environmental changes and transcriptional regulation to start acclimation processes.

EXPERIMENTAL PROCEDURES

Strains and Culture Conditions - A glucose-tolerant wild-type strain of *Synechocystis* sp. PCC 6803 was grown at 32ºC in BG-11 medium with 20 mM Hepes-NaOH, pH 7.0, under continuous illumination at 20 μmol photons m^{-2} s^{-1} with bubbling of air. The ssl0564-disrupted mutant was grown under the same condition, except that 20 μg/ml kanamycin sulfate was added to the medium. Cell density was estimated as A_{730} with a spectrophotometer (model UV-160A; Shimadzu). High-light shift experiments were performed by transferring cells at the exponential growth phase (A_{730} = 0.1 to 0.2) from low-light (20 μmol photons m^{-2} s^{-1}) to high-light (300 μmol photons m^{-2} s^{-1}) conditions.

Construction of the ssl0564-disrupted mutant - Gene-flanking segment of ssl0564 (1000 bp) was amplified by PCR using primers 0564delF (5'-ACCGAGGATTGTGTTGG-3') and 0564delR (5'-ATGATCACGGGGAATGCG-3'), and cloned into pT7Blue T-vector (Novagen). A kanamycin-resistance cartridge, which had been excised from the plasmid pRL161 by digestion with *Hin*cII, was inserted into the coding region of ssl0564 at the *Apa*I site. Wild-type cells were transformed with the construct and transformants were selected by 20 μg/ml kanamycin sulfate. The complete segregation of the mutant genome was verified by PCR.

RT-PCR analysis - To examine the expression level of ssl0564, 0564F (5'-AACATATGCTGGCCGGGAACTAT-3') and 0564R (5'-AAGGATCCTAAGACCCACTGCCTTG-3') were used as RT-PCR primers. RT-PCR reaction was performed by using mRNA Selective PCR kit Ver. 1.1 (Takara). Amplified products were electrophoretically examined on 1% agarose gels.

DNA microarray analysis - Total RNA used for DNA microarray analysis was isolated using the RNeasy Midi kit (Qiagen) as previously described (6). After the removal of trace amounts of contaminating genomic DNA by treatment with DNase I (Takara), RNA was labeled with Cy3-dUTP or Cy5-dUTP (Amersham Pharmacia) using RNA fluorescence labeling core kit Ver. 2.0 (M-MLV version; Takara). Hybridization of labeled cDNAs with CyanoCHIP (ver. 1.6; Takara) was performed according to the manufacturer's instruction. Image acquisition with a ScanArray 4000 (GSI Lumonics) and data analysis by a QuantArray version 2.0 software (GSI Lumonics) were performed as previously described (16).

RNA gel blot analysis - Isolation of RNA by the hot-phenol method and RNA gel blot analyses, using DIG RNA Labeling and Detection kit (Roche), were performed as previously described (18). To generate RNA probes by *in vitro* transcription, template DNA fragments for *ndhD2*, *rpe* and slr1957 probes were amplified using the following primers: *ndhD2*-F (5'-AACGTACGAGCCGAATTCTACTGGTA-3') and T7-*ndhD2*-R (5'-TAATACGACTCACTATAGGGCGA CAGTAGGAGCATGTCCT-3'), *rpe*-F (5'-TAAAAAGTAGGCTTAAAT-3') and T7-*rpe*-R

(5'-TAATACGACTCACTATAGGGCGATTAACGCTCATGATCA -3'), slr1957-F (5'-ATGAGACATTTTTGCGAC-3') and T7-slr1957-R (5'-TAATACGACTCACTATAGGGCGA TTAAATTTCTTCCATCTC-3'). Nucleotide sequences underlined indicate T7 polymerase recognition site added to the reverse primers at their 5'-termini. PCR products were directly used as templates for *in vitro* transcription reaction.

Overexpression and Purification of Ssl0564 - The ssl0564 coding region was PCR-amplified by using primers 0564F (5'-AACATATGCTGGCCGGGAACTAT-3') and 0564R (5'-AAGGATCCTAAGACCCACTGCCTTG-3'), cloned into pT7Blue T-Vector (Novagen), digested with *Nde*I and *Bam*HI (sites underlined), and subcloned into the same restriction sites in pET28a (Novagen) to create pET0564 for expression of a fusion protein with N-terminal His-tag. The nucleotide sequence was confirmed by DNA sequencing using the BigDye terminator method (Applied Biosystems). *Escherichia coli* BL21(DE3) harboring pET0564 was grown in 800 ml culture containing 20 μg/ml kanamycin sulfate for 9 h at 37ºC without addition of isopropyl β-D-thiogalactoside. Cells were harvested by centrifugation, resuspended in 15 ml of 20 mM phosphate buffer, pH7.4, containing 0.5 M NaCl and 60 mM imidazole and disrupted by sonication for 30 sec for 10 times at 4ºC. After the removal of unbroken cells and insoluble materials by centrifugation, the soluble protein fraction was filtrated through a 0.2 μm filter (DISMIC-25cs; ADVANTEC). His-Ssl0564 was purified by nickel affinity column chromatography using a HiTrap Chelating HP column (Amersham Biosciences). The soluble protein fraction was applied to the column equilibrated with 20 mM phosphate buffer, pH7.4, containing 0.5 M NaCl and 60 mM imidazole, washed with the same buffer and eluted with 20 mM phosphate buffer, pH7.4, containing 0.5 M NaCl and 200 mM imidazole. Purified His-Ssl0564 was desalted by a HiTrap Desalting column (Amersham Biosciences). Protein composition was examined by electrophoresis in a non-reducing 15% SDS-polyacrylamide gel followed by staining with Coomassie Brilliant Blue R-250.

Gel mobility shift assay - For preparation of the probes and the specific competitor DNA fragments for gel mobility shift assays, the following DNA fragments corresponding to the promoter region of each gene were obtained by PCR amplification: ssl0564 (from nucleotide 2287333 to 2287068 according to numbering in CyanoBase), *ndhD2* (from nucleotide 285939 to 286163), *rpe* (from nucleotide 1713448 to 1713257), *chlL* (from nucleotide 3415526 to 3415988), slr1957 (from nucleotide 1755153 to 1755591), *chlB* (from nucleotide 2394872 to 2395102) and *psaD* (from nucleotide 126444 to 126638). The 3' end of DNA fragment for the probe was labeled with DIG-ddUTP by the terminal transferase according to manufacturer's instructions (DIG Gel Shift kit; Roche). Assays were performed using DIG Gel Shift kit according to manufacturer's instructions. Purified His-Ssl0564 protein was incubated with 30 fmol DIG-labeled DNA fragment in a 20 μl reaction mixture containing 1 μg poly d[I-C], 0.1 μg poly L-lysine, 20 mM Hepes-KOH, pH 7.6, 1 mM EDTA, 10 mM $(NH_4)_2SO_4$, 0.2% (w/v) Tween 20, and 30 mM KCl. After incubation overnight at room temperature, 5 μl of gel loading buffer consisting of 60% (v/v) of 1×TBE and 40% (v/v) glycerol was added to the reaction mixture. Samples were then applied onto a 6% polyacrylamide gel and subjected to electrophoresis at 95 V for 2.5 h at 4°C. DNA and protein were transferred to a nylon membrane (Hybond N+; Amersham Biosciences) by capillary transfer method and fixed by baking at 80°C for 2 h. Detection of DIG-labeled probe was performed according to the standard protocol for DIG Luminescent Detection kit (Roche).

Immunoblot analysis - 50 ml of cell cultures at A_{730}=0.1 were mixed with 5 ml of 100% trichloroacetic acid (TCA). Cells were collected by centrifugation, resuspended with 15 μl of 10% TCA/ 0.1% SDS and incubated at 4ºC for 1 h. Alkylation of samples was performed by addition of 15 μl of 2 x *N*-ethylmaleimide (NEM) buffer (300 mM Tris-HCl, pH9.0/ 0.5% SDS/ 10 mM NEM) or 15 μl of 2 x 4-acetamido-4'-maleimidylstilbene-2,2'-disulfonic acid (AMS) buffer (300 mM Tris-HCl, pH9.0/ 0.3% SDS/ 30 mM AMS). After addition of enough amount of 1.5 M Tris-HCl, pH9.0, for

neutralization, samples were incubated at 37ºC for 2 h. Alkylated samples were separated by non-reducing 15% SDS-polyacrylamide gel electrophoresis with 8 M urea, blotted to PVDF membrane (Immobilon-P; Millipore) and probed with polyclonal antibodies to His-Ssl0564 recombinant protein. The bound antibodies were detected with goat anti-rabbit IgG secondary antibodies conjugated to alkaline phosphatase.

RESULTS

Small LuxR-type regulators are highly conserved among cyanobacterial species

In this study, we initiated the characterization of a small LuxR-type regulator (SLTR), Ssl0564, in a cyanobacterium *Synechocystis* sp. PCC 6803. The LuxR subfamily is one of the major groups of bacterial transcriptional regulatory proteins that bind DNA via a helix-turn-helix (HTH) motif. It includes a large number of proteins consisting of two domains: a C-terminal DNA-binding domain with a HTH motif, and an N-terminal receiver domain that can be activated by either phosphorylation or binding of an effector molecule (19, 20). In addition, there exists a small group of SLTRs consisting solely of a DNA-binding domain. SLTRs, about 100 amino acid residues in length, are found in a wide range of bacteria such as proteobacteria, firmicutes and cyanobacteria (http://smart.embl-heidelberg.de/). They have not been characterized yet except for GerE that functions in *Bacillus subtilis* at the late stages of sporulation (21, 22, 23).

Figure 1 shows the phylogenetic tree of SLTRs constructed with the neighbor-joining algorithm. It is noticeable that most of the cyanobacterial SLTRs form a discrete clade (shown in gray). All the cyanobacterial species for which the genomic sequencing has been completed possess one SLTR in this clade. The notable feature of SLTRs in the cyanobacterial clade is recognized in the C-terminal extension containing three conserved cysteine residues (Fig. 2). This region is only conserved in cyanobacterial subfamily in SLTRs suggesting that it may be involved in regulatory mechanisms characteristic of photosynthetic organisms. Several cyanobacterial species such as *Gloeobacter violaceus*, *Synechococcus* sp. WH8102 and *Prochlorococcus marinus* MIT9313 have multiple SLTRs. In such cases, only one regulator is in the cyanobacterial clade whereas the other SLTRs are rather divergent and do not have three cysteine residues unique to SLTRs in the cyanobacterial clade.

Ssl0564 acts as both a positive and a negative regulator

RT-PCR analysis suggested that ssl0564 is weakly expressed in cells of *Synechocystis* sp. PCC 6803 incubated under the dark, low-light (20 μmol photons m^{-2} s^{-1}) and high-light (300 μmol photons $m^{-2}s^{-1}$) conditions (not shown). To investigate the physiological role of Ssl0564, first we made a gene-disrupted mutant of ssl0564 (the Δssl0564 mutant) by the insertion of a kanamycin-resistance cartridge. The growth characteristics of the Δssl0564 mutant were similar to that of the wild-type strain under all growth conditions examined, including low light, high light, high temperature (42ºC), and presence of ethanol (3%), glucose (5 mM) or NaCl (0.4 M) (not shown).

To identify target genes of Ssl0564, we compared the gene expression profiles in the wild-type and the Δssl0564 mutant cells under low-light conditions by DNA microarray analysis (Fig. 3). Most genes were similarly expressed in both strains but the transcript levels of several genes were reproducibly affected by the disruption of ssl0564 (Table 1). It was suggested that Ssl0564 represses the transcription of *ndhD2*, *rpe* and the ssl0564-sll0296 operon and activates that of *chlL*, *chlN*, *chlB*, and slr1957 under low-light conditions.

Ssl0564 becomes a dimeric form through the formation of intermolecular disulfide bond(s)

To characterize the gene product of ssl0564, His-tagged Ssl0564 expressed in *E. coli* was purified by nickel affinity column chromatography and used for subsequent analyses. When the purified protein was subjected to non-reducing SDS-PAGE, we observed two bands with molecular mass of 12 kDa and 24 kDa (Fig. 4A, lanes 2 and 9). Treatment of Ssl0564 with oxidizing agents such as potassium ferricyanide (lane 3), thiol-specific oxidant, diamide (lane 4) or hydrogen peroxide (lane 5) resulted in a significant rise in the intensity of the 24 kDa band at the expense of the 12 kDa band. Subsequent treatments of the oxidized Ssl0564, which had been treated by

hydrogen peroxide, with reducing agents such as DTT (lane 6), β-mercaptoethanol (lane 7) or reduced form of glutathione (lane 8) reversed the relative abundances of these bands. These results suggested that Ssl0564 undergoes dimerization under oxidizing conditions *in vitro*. To examine the possibility that dimerization occurs via the formation of intermolecular disulfide bond(s), we treated Ssl0564 with a thiol-alkylating reagent, *N*-ethylmaleimide (NEM), before incubation with hydrogen peroxide (Fig. 4B). The alkylated Ssl0564 could no longer form dimer (lane 4), suggesting that the formation of intermolecular disulfide bond(s) is essential for dimerization.

Dimeric form of Ssl0564 can bind to the promoter region of its target genes

To test whether genes listed in Table 1 are indeed targets of Ssl0564, we performed DNA gel mobility shift assay of the promoter segments of these genes with purified His-Ssl0564 protein in the presence of potassium ferricyanide (Fig 5A). Although clear shifted bands were not observed, the intensity of the band corresponding to the free probe (lane 1) decreased with the increase of Ssl0564 protein in the reaction mixture (lanes 2-4). It is notable that the addition of non-labeled competitor DNA together with Ssl0564 protein could suppress the decrease of the free probe band (lane 5). When the promoter segment of *psaD*, which does not function as a target gene, was used as a probe, the band pattern was not affected by the addition of Ssl0564 protein. These data supported the notion that specific complexes were formed between Ssl0564 and promoter segments of putative target genes.

Next, we tested the binding ability of Ssl0564 protein in various redox environments. In Figure 5B, the binding activity of Ssl0564 protein to *ndhD2* probe was examined without redox agents (lane 2), in the presence of the oxidizing agent, ferricyanide (lane 3) or in the presence of the reducing agent, DTT (lane 4). Although Ssl0564 could bind to *ndhD2* probe in the absence of redox agents, oxidizing environment promoted the formation of the complex of Ssl0564 with *ndhD2* probe. On the other hand, addition of DTT prevented the formation of such a complex. When *ndhD2* probe was incubated with ferricyanide or DTT in the absence of Ssl0564 protein, no changes in band pattern was observed (lane 5-7). These results indicate that dimerization is prerequisite for stable binding of Ssl0564 to its target sequences.

Transcriptional regulation by Ssl0564 is achieved depending on the activity of photosynthetic electron transport

We then followed the transcript levels of *rpe*, *ndhD2*, and slr1957 in the wild-type and the Δssl0564 mutant under different light conditions by RNA gel blot analysis (Fig. 6). Under low-light conditions, the level of the transcripts originating from *rpe* and *ndhD2* was low in the wild-type cells (lane 1), whereas such a down-regulation was fully (*rpe*) or partially (*ndhD2*) abolished in the mutant (lane 2). In the case of slr1957, its transcript was highly accumulated in the wild-type (lane 1) and was scarcely observed in the mutant (lane 2). These observations agree with the results of DNA microarray analysis showing that Ssl0564 acts as a negative regulator for *rpe* and *ndhD2*, and a positive regulator for slr1957 under low-light conditions. Within 15 min after the shift to high-light conditions, increase of *rpe* and *ndhD2* transcripts and decrease of slr1957 transcript were observed in the wild-type cells (lane 3), showing that light response of these genes is attained by the inactivation of Ssl0564 under high-light conditions. As expected, in the Δssl0564 mutant, high-light response of these genes was much less prominent than that in the wild-type cells (lane 4).

Then, which is the critical factor for Ssl0564-dependent transcriptional regulation, changes in photon flux density *per se* or those in the redox state of the photosynthetic electron transport chain? To answer this question, 3-(3,4-dichlorophenyl)-1,1-dimethylurea (DCMU) or methyl viologen was added to cultures upon the shift to high-light conditions. By the addition of DCMU or methyl viologen, the supply of reducing equivalents from the photosynthetic electron transport chain to stromal components is perturbed even under high-light conditions because DCMU and methyl viologen inhibit electron transfer from photosystem II to the plastoquinone pool and that from photosystem I to ferredoxin, respectively (24, 25). In the presence of these reagents, induction of *rpe* and *ndhD2* and repression of slr1957 were hardly observed in the wild-type cells upon the shift to high-light conditions (lanes 5 and 7). The only exception

was marked down-regulation of slr1957 treated with methyl viologen, which may be attributed to unidentified regulatory factors other than Ssl0564. In the case of the Δssl0564 mutant, the transcript levels of the target genes were not affected by the addition of DCMU or methyl viologen (lanes 6 and 8). Above observations clearly indicate that Ssl0564 works as a transcriptional regulator under the conditions where the activity of the photosynthetic electron transport is low and supply of reducing equivalents is limited, e.g., low-light conditions.

Ssl0564 protein undergoes conformational change depending on the activity of photosynthetic electron transport

To elucidate the mechanism by which the activity of Ssl0564 is modulated, we examined the physiological state of Ssl0564 *in vivo* by immunoblot analysis. The wild-type cultures were incubated under the same conditions used for RNA gel blot analysis shown in Figure 6. After cultures were treated with 10% TCA to fix cellular proteins, thiols were alkylated by NEM or AMS to inhibit their non-specific interaction, which is an essential step for successful detection of Ssl0564. Then the proteins were separated by non-reducing SDS-PAGE and Ssl0564 was detected using its specific antibody. As shown in Figure 7, we observed that the constant amount of Ssl0564 exists in *Synechocystis* cells exclusively as a dimeric form both under low- and high-light conditions. It thus appears that neither oligomeric state nor amount of Ssl0564 is critical for the light-dependent regulation of its activity *in vivo*.

Unexpectedly, we observed that the dimeric form of Ssl0564 was separated into two bands (Fig. 7). In low-light grown cell extracts, the fast migrating band was mainly detected (lane 2). Exposure of cells to high light for 15 min resulted in significant increase of the slowly migrating band (lane 3). On the other hand, in extracts of cells incubated with DCMU or methyl viologen during the high-light treatment, only the fast migrating band was detected (lanes 3 and 4), indicating that elevation of photosynthetic electron transport activity upon the shift to high light caused the increase in the relative intensity of the slowly migrating band. Furthermore, these data, together with the results of RNA gel blot analysis (Fig. 6), suggest that the slowly or fast migrating band corresponds to the inactive or active form of Ssl0564, respectively. It must be noted that alkylation of samples with either NEM or AMS gave the same pattern of band shift (not shown). If Ssl0564 has any free thiol groups, the addition of AMS moiety (500 Da) per a thiol would cause larger band shift than the addition of NEM moiety (125 Da). The band shift of Ssl0564 independent of alkylating agents indicates that three cysteine residues in Ssl0564 are always in oxidized form and the conformational change of Ssl0564 is not due to redox active cysteines.

The upshift of photon flux density causes transient inactivation of Ssl0564.

We examined the time-course change of the conformation of Ssl0564 and expression level of its target genes, *rpe*, *ndhD2* and slr1957 upon the shift to high-light conditions (Fig. 8). Within 5 min after the shift to high light, most of the Ssl0564 protein turned into the inactive form with slower electrophoretic mobility, which was followed by the accumulation of *ndhD2* and *rpe* transcripts and the disappearance of slr1957 transcript. After the temporal increase of the inactive form, the active form of Ssl0564 with faster electrophoretic mobility increased again.

Next, cell cultures grown at photon flux density of 20 μmol photons m^{-2} s^{-1} were exposed to different level of illumination for 5 min. As shown in Figure 9A, upshift of photon flux density over 100 μmol photons m^{-2} s^{-1} resulted in the significant increase of the slowly migrating form, i.e., the inactive form of Ssl0564. As expected, this change in conformation of Ssl0564 was accompanied by the induction of *ndhD2* and *rpe* and the repression of slr1957 (Fig. 9B). Several repeats of similar experiments indicated that the threshold for the inactivation of Ssl0564 exists around 60 - 80 μmol photons m^{-2} s^{-1}.

As mentioned in Introduction, the redox state of the plastoquinone pool is recognized as a critical factor for transcriptional regulation of photosynthesis-related genes. To check the possibility that the activity of Ssl0564 is modulated by the redox state of the plastoquinone pool, we compared the effect of addition of two photosynthetic inhibitors: DCMU and 2,5-dibromo-3-methyl-6-isopropyl-*p*-benzoquinone (DBMIB) that inhibits electron transport from the plastoquinone pool to cytochrome b_6f complex. These two inhibitors have opposite effects on the net redox state of the plastoquinone pool: more oxidized in the presence of DCMU and more reduced in the presence of DBMIB (24).

Upon the shift to high-light conditions, both inhibitors completely suppressed the appearance of the inactive form of Ssl0564 together with the light response of its target genes (Fig. 10), indicating that activity of Ssl0564 is regulated irrespective of the redox state of the plastoquinone pool.

DISCUSSION

Transcriptional regulation by PedR coupled with the activity of photosynthetic electron transport

In this study, we show that one of cyanobacterial orthologs of SLTR, Ssl0564, works as a sensor of photosynthetic activity and achieves the photon flux density-dependent transcriptional regulation of a set of genes in *Synechocystis* sp. PCC 6803. Thus, we propose that Ssl0564 is designated PedR (Photosynthetic Electron transport Dependent Regulator).

Upon the transfer of the wild-type cultures from low- to high-light conditions, we observed the inactivation (Fig. 6) and the conformational change (Fig. 7) of PedR. Addition of DCMU, DBMIB or methyl viologen extinguished the effect of the upshift of photon flux density (Figs. 6, 7 and 10), indicating that the activity of the photosynthetic electron transport rather than photon flux density *per se* is critical for the regulation of PedR activity. Considering that similar results were obtained by the addition of these reagents, which perturb different points of photosynthetic electron transport chain, the activity of PedR is likely to be modulated by the availability of reducing equivalents provided at the acceptor side of photosystem I (Fig. 11). Under low-light conditions where activity of the photosynthetic electron transport is low, a large fraction of PedR is in the active compact form and regulates expression of its target genes. Upon the sudden elevation of photon flux density, supply of reducing equivalents from photosynthetic electron transport chain abruptly increases, leading to the conformational change and inactivation of PedR. As the acclimation responses take place to mitigate the over-reduction of photosynthetic electron transport chain, PedR returns to the active form again. This mechanism seems to enable transient induction or repression of the target genes in response to sudden changes in photon flux density.

The physiological significance of transcriptional regulation by PedR

It is notable that genes involved in various cellular functions are coordinately regulated by PedR (Table 1). When the activity of photosynthetic electron transport is low, PedR positively regulates the expression of *chlL*, *chlN* and *chlB* encoding subunits of light-independent protochlorophyllide reductase and an uncharacterized ORF, slr1957. Upon the upshift of photon flux density, transcription of these genes is down-regulated due to the inactivation of PedR. DNA microarray analysis showed that genes involved in biosynthesis of photosynthetic pigments including *chlL*, *chlN* and *chlB* were remarkably down-regulated under high-light conditions (6). This is quite reasonable considering that absorption of excess light energy should be avoided under high-light conditions. PedR seems to take a part in this acclimation response. As for slr1957, its physiological role is totally unknown. Judging from its expression pattern, it may have some roles under dark or low-light conditions. We observed that expression of slr1957 is sometimes not fully activated under the conditions where PedR is in the active state (Fig. 6, HL+MV; Fig.9, 20 μmol photons m^{-2} s^{-1}). There must be a negative regulation of slr1957 by a certain factor, in addition to the positive regulation by PedR.

Transcription of *ndhD2*, *rpe* and *pedR*-sll0296 operon is negatively regulated by PedR under low-light conditions and derepressed upon the sudden increase of photosynthetic electron transport activity. *ndhD2* is one of six *ndhD* genes in *Synechocystis* sp. PCC 6803 and encodes NdhD2 subunit involved in electron transport from NADPH to the plastoquinone pool (26). This gene was remarkably up-regulated under high-light conditions (6). Although the precise role of NdhD2 subunit has not been identified, it may contribute to cycling of excess reducing equivalents under high-light conditions. Tu et al. reported that a sensor histidine kinase, Hik33 (DspA) is involved in the repression of *ndhD2* under low-light conditions (8). This well agrees with our observation that the expression of *ndhD2* was not fully derepressed in the Δssl0564 mutant exposed to low-photon flux density. Hik33 and PedR may belong to independent pathways of signal transduction for light response of *ndhD2* gene. Another gene

negatively regulated by PedR, *rpe*, encodes pentose-5-phosphate-3-epimerase that catalyses the interconversion of ribulose-5-phosphate and xylulose-5-phosphate in the Calvin cycle and in the oxidative pentose phosphate pathway. Although this enzyme in cyanobacteria has not been characterized, it is plausible that expression level of *rpe* has some regulatory role on cellular metabolism. It was shown that PedR binds to its own promoter to repress the transcription of *pedR* itself and sll0296 locating just downstream of *pedR*. The transcript level of *pedR* is maintained at low level irrespective of the growth condition, which seems to be attained by negative autoregulation.

The structural characteristics of PedR

Among SLTRs conserved in many bacterial species, only GerE in *Bacillus subtilis* has been extensively characterized and its crystal structure was solved at 2.05 Å resolution (23). Comparison of the structure of cyanobacterial SLTRs with that of GerE may provide additional insights into the function of cyanobacterial SLTRs. GerE consists of four α-helices: the central pair, α-2 and α-3, forms a HTH motif whereas α-4 in the C-terminal region is involved in dimerization. These α-helices, especially the central pair involved in DNA binding, are well-conserved in cyanobacterial SLTRs (Fig. 2), suggesting that the DNA binding mechanism of PedR is similar to that of GerE. In the promoter regions of target genes of PedR, there found multiple inverted repeats, consisting of the 12-mer sequence 5'-RWWTRGGYNNYY-3', typical of GerE-binding motifs. It has been shown that the positioning and multiplicity of GerE binding sites are variable (23) and GerE can act both as a positive and as a negative regulator depending on its binding position (27). By similar mechanism, PedR could work for positive or negative regulation. When we examined the binding ability of His-PedR to the promoter regions of its putative target genes, distinct shifted band was not observed in most cases (Fig. 5). This is probably due to the heterogeneous population of His-PedR-DNA complex. Variable number of His-PedR bound to multiple binding sites located on a promoter fragment, which may result in a smearing of the shifted band.

SLTRs in the cyanobacterial clade (Fig. 1) have unique C-terminal region not conserved in any other bacterial SLTRs (Fig. 2). The region extends from α-4 helix and contains three conserved cysteine residues. Characterization of His-PedR protein suggested that some of these cysteines are involved in dimerization through the formation of intermolecular disulfide bond(s) (Fig. 4). By the addition of reducing agents, PedR becomes monomeric form *in vitro* (Fig. 4) and also *in vivo* (not shown). Under physiological conditions, however, PedR constitutively exists as a dimer and the monomeric form was scarcely observed (Fig. 7). It seems that the supply of reducing equivalents from photosynthetic electron transport chain is not strong enough to reduce the intermolecular disulfide bond(s) but is sufficient for the observed conformational change, which is presumably critical for the regulation of the PedR activity. The nature of the conformational change has not been identified. Three cysteine residues were insensitive to AMS modification, indicating that they are constitutively in the oxidized form and not responsible for the redox-dependent conformational change of PedR. Temporal modification of a certain amino acid residue could occur upon the supply of reducing equivalents, leading to the conformational change and inactivation of PedR. To identify the amino acid residues critical for the regulation of PedR activity, we are now trying to introduce random amino acid substitution into PedR protein and examine the consequence of the mutagenesis.

REFERENCES

1. Huner, N.P.A., Oquist, G., and Sarhan, F. (1998) *Trends Plant Sci*. **3**, 224–230
2. Anderson, J.M. (1986) *Annu. Rev. Plant Physiol.* **3**, 93-136
3. Hihara, Y. (1999) *Curr. Top. Plant Biol.* **1**, 37-50
4. Bailey, S., Horton, P., and Walters, R.G. (2004) *Planta* **218**, 793-802

5. Asada, K. (1994) in *Causes of photooxidative stress and amelioration of defense systems in plants* (Foyer, C.H., and Mullineaux, P.M., eds) pp.77-104
6. Hihara,Y., Kamei, A., Kanehisa, M., Kaplan, A., and Ikeuchi, M. (2001) *Plant Cell* **13**, 793-806
7. Huang, L., McCluskey, M.P., Ni, H., and LaRossa, R.A. (2002) *J. Bacteriol.* **184**, 6845-6858
8. Tu, C.-J., Shrager, J., Burnap, R.L., Postier, B.L., and Grossman, A.R. (2004) *J. Bacteriol.* **186**, 3889-3902
9. Suzuki, I., Kanesaki, Y., Mikami, K., Kanehisa, M., and Murata, N. (2001) *Mol. Microbiol.* **40**, 235-244
10. Kanesaki, Y., Suzuki, I., Allakhverdiev, S.I., Mikami, K., and Murata, N. (2002) *Biochem. Biophys. Res. Comm.* **290**, 339-348
11. Wang, H.-L., Postier, B.L., and Burnap, R.L. (2004) *J. Biol. Chem.* **279**, 5739-5751
12. Li, H., Singh, A.K., McIntyre, L.M., and Sherman, L.A. (2004) *J. Bacteriol.* **186**, 3331-3345
13. Singh, A.K., McIntyre, L.M., and Sherman, L.A. (2003) *Plant Physiol.* **132**, 1825-1839
14. Durnford, D.G., and Falkowski, P.G. (1997) *Photosynth. Res.* **53**, 229–241
15. Allen, J.F., and Pfannschmidt, T. (2000) *Philos. Trans. R. Soc. Lond. B Biol. Sci.* **355**, 1351-1359
16. Hihara, Y., Sonoike, K., Kanehisa, M., and Ikeuchi, M. (2003) *J. Bacteriol.* **185**, 1719-1725
17. Piippo, M., Allahverdiyeva, Y., Paakkarinen, V., Suoranta, U.M., Battchikova, N., and Aro, E.M. (2006) *Physiol. Genomics* **25**, 142-152
18. Muramatsu, M., and Hihara, Y. (2003) *Planta* **216**, 446-453
19. Pao, G.M., Tam, R., Lipschiz, L.S., and Saier, J. (1994) *Res. Microbiol.* **145**, 356-362
20. Danot, O., Vidal-Ingigliardi, D., and Raibaud, O. (1996) *J. Mol. Biol.* **262**, 1-11
21. Cutting, S., Panzer, S., and Losick, R. (1989) *J. Mol. Biol.* **207**, 393-404
22. Zheng, L., Halberg, R., Roels, S., Ichikawa, H., Kroos, L., and Losick, R. (1992) *J. Mol. Biol.* **226**, 1037-1050
23. Ducros, V.M.-A., Lewis, R.J., Verma, C.S., Dodson, E.J., Leonard, G., Turkenburg, J.P., Murshudov, G.N., Wilkinson, A.J., and Brannigan, J.A. (2001) *J. Mol. Biol.* **306**, 759-771
24. Trebst, A. (1980) *Methods Enzymol.* **69**, 675-715
25. Izawa, S. (1980) *Methods Enzymol.* **69**, 413-433
26. Ohkawa, H., Pakrasi, H.B., and Ogawa, T. (2000) *J. Biol. Chem.* **275**, 31630-31634
27. Ichikawa, H., Halberg, R., and Kroos, L. (1999) *J. Biol. Chem.* **274**, 8322-8327

FOOTNOTES

We thank Prof. Aaron Kaplan and Prof. Kintake Sonoike for critical reading of the manuscript and Ms. Mayumi Horiuchi for her assistance in Immunoblot analysis. This work was financially supported by a Grant-in-Aid for Young Scientists from the Ministry of Education, Culture, Sports, Science and Technology of Japan (to Y. H.).

The abbreviations used are: AMS, 4-acetamido-4'-maleimidylstilbene-2,2'-disulfonic acid; DBMIB, 2,5-dibromo-3-methyl-6-isopropyl-*p*-benzoquinone; DCMU, 3-(3,4-dichlorophenyl)-1,1-dimethylurea; HTH, helix-turn-helix ; NEM, *N*-ethylmaleimide; TCA, trichloroacetic acid

FIGURE LEGENDS

Fig. 1 Unrooted phylogenetic tree of small LuxR-type transcriptional regulators generated with the neighbor-joining algorithm. Protein sequences of bacterial small LuxR-type transcriptional regulators were retrieved mainly from SMART database (http://smart.embl-heidelberg.de/; *Bacillus subtilis* (GerE) [P11470], *Pseudomonas syringae* [Q87WB0], *Bordetella bronchiseptica* [Q7WES5], *Prochlorococcus marinus* MIT9313 (PMT0867) [Q7V787], *Rhizobium loti* [Q98EY1], *Pseudomonas solanacearum* [Q8XQN0], *Gloeobacter violaceus* (Glr0352) [Q7NNQ8], *Gloeobacter violaceus*

(Gsr1799) [Q7NJN3], *Xanthomonas campestris* [Q8PEB0], *Thermoanaerobacter tengcongensis* [Q8R6P6], *Bacillus cereus* [Q81DC6], *Salmonella typhimurium* [Q04825], *Agrobacterium tumefaciens* [Q8UIX6], *Yersinia pestis* [Q9RPN2], *Prochlorococcus marinus* MIT9313 (PMT1655) [Q7V5B4], *Synechococcus* sp.WH8102 (SYNW1973) [Q7U4U0], *Coxiella burnetii* [Q83AD2], *Anabaena* sp. PCC 7120 (Asl2551) [Q8YU10], *Synechocystis* sp. PCC 6803 (Ssl0564) [Q55540], *Synechococcus* sp. PCC 7942 [ZP_00165254], *Thermosynechococcus elongatus* (Tsl1865) [Q8DHT0], *Gloeobacter violaceus* (Gsl4037) [Q7NE43], *Prochlorococcus marinus* MIT9313 (PMT2014) [Q7V4E0], *Prochlorococcus marinus* SS120 (Pro0177)[Q7VE37], *Prochlorococcus marinus* MED4 (PMM0154) [Q7V3C4], *Synechococcus* sp.WH8102 (SYNW2268) [Q7U408]). The unrooted phylogenetic tree was generated and displayed by ClustalW program at GenomeNet of Kyoto University (http://clustalw.genome.jp/).

Fig. 2 The amino-acid sequences of cyanobacterial SLTRs aligned against those of divergent SLTRs in cyanobacteria and those of SLTRs in other bacterial species. Amino acid residues conserved among at least six cyanobacterial SLTRs are shown in black. Gray areas denote similar amino acid residues. Astarisks placed above the sequence of Ssl0564 indicate cysteine residues conserved among cyanobacterial SLTRs. Location of four α-helices characterized in GerE is shown below the sequences.

Fig. 3 Effect of the disruption of ssl0564 gene on the global gene expression profile shown by scatter plots. Gene expression profile under low-light conditions was compared between the wild-type cells and the Δssl0564 mutant. Signal intensities of 6148 spots (3074 ORFs in duplicate) were plotted. Solid lines indicate the limit of experimental deviations (50% deviation). Symbols show the signal intensities of duplicate spots of putative target genes of Ssl0564. double cycle: ssl0564, open cycle: sll0296, open square: *rpe*, open diamond: *ndhD2*, double square: *chlL*, double diamond: *chlN*, double triangle: *chlB*, open triangle: slr1957.

Fig. 4 Effect of oxidizing-, reducing- or thiol modifying-agents on the oligomeric state of the recombinant Ssl0564 protein. (A) 5 μg of His-Ssl0564 was incubated with various oxidizing- or reducing-agents and then separated by non-reducing 15% SDS-polyacrylamide gel electrophoresis. Lane 1, Molecular mass standard marker (kDa). Lanes 2 and 9, His-Ssl0564 without additives. Lane 3-5, His-Ssl0564 incubated overnight with 100 μM ferricyanide, with 1 mM diamide or with 1 mM hydrogen peroxide, respectively. Lane 6-8, His-Ssl0564 incubated with 1 mM hydrogen peroxide overnight and then treated with 1 mM DTT for 1 h, with 5% β-mercaptoethanol for 1 h or with 10 mM reduced form of glutathione for 20 h, respectively. (B) 5 μg of His-Ssl0564 was treated with (Lane 3 and 4) or without (Lane 1 and 2) 5 mM NEM for 2 h, further incubated with (Lane 2 and 4) or without (Lane 1 and 3) 1 mM hydrogen peroxide overnight and then separated by non-reducing 15% SDS-polyacrylamide gel electrophoresis.

Fig. 5 Gel mobility shift assays of the promoter segments of the putative target genes with purified His-Ssl0564. (A) DIG-labeled promoter segment of each gene was incubated overnight with purified His-Ssl0564 added at increasing concentrations (0 μg for Lane 1, 0.04 μg for Lane 2, 0.4 μg for Lane 3 and 4 μg for Lanes 4 and 5) in the presence of 100 μM ferricyanide. For Lane 5, 300-fold-excess amounts of the non-labeled promoter segment was added as a competitor. (B) DIG-labeled promoter segment of *ndhD2* was incubated overnight with purified His-Ssl0564 under various redox conditions. Lane 1, *ndhD2* probe without additives. Lanes 2-4, *ndhD2* probe and 1 μg of His-Ssl0564 incubated without redox agents, with 100 μM ferricyanide or with 1 mM DTT, respectively. Lanes 5-7, *ndhD2* probe incubated without redox agents, with 100 μM ferricyanide or with 1 mM DTT, respectively.

Fig. 6 RNA gel blot analysis of the expression of the *rpe*, *ndhD2* and slr1957 genes in the wild-type and the Δssl0564 mutant. Total RNA was isolated from cells incubated under following conditions: low-light conditions (LL), high-light conditions for 15 min (HL), HL conditions with 10

μM DCMU for 15 min (HL+DCMU) or HL conditions with 10 μM methyl viologen for 15 min (HL+MV). 2 μg of total RNA per a lane was loaded for the detection of *rpe* and *ndhD2* transcripts and 6 μg was loaded for slr1957 transcript.

Fig. 7 Examination of physiological state of Ssl0564 *in vivo*. TCA fixed proteins from cells incubated under low-light conditions (LL), high-light conditions for 15 min (HL), HL conditions with 10 μM DCMU for 15 min (HL+DCMU) or HL conditions with 10 μM methyl viologen for 15 min (HL+MV) were alkylated and 6.8 μg of total protein per a lane was separated by non-reducing 15% SDS-polyacrylamide gel electrophoresis with 8 M urea. For comparison, 30 ng of His-Ssl0564 was also electrophoresed. Ssl0564 was detected by its specific antibody.

Fig. 8 Time course change of the conformation of Ssl0564 and the expression level of its target genes, *rpe*, *ndhD2* and slr1957, upon the shift to high-light conditions. (A) TCA fixed proteins from cells incubated under high light were alkylated and 7.5 μg of total protein per a lane was separated by non-reducing 15% SDS-polyacrylamide gel electrophoresis with 8 M urea. Ssl0564 was detected by its specific antibody. (B) Total RNA was isolated from cells incubated under high-light conditions. 2 μg of total RNA per a lane was loaded for the detection of *rpe* and *ndhD2* transcripts and 6 μg was loaded for slr1957 transcript.

Fig. 9 Photon flux density dependence of the conformational change of Ssl0564 and the expression level of its target genes, *rpe*, *ndhD2* and slr1957. (A) TCA fixed proteins from cells exposed to various level of illumination for 5 min were alkylated and 4 μg of total protein per a lane was separated by non-reducing 15% SDS-polyacrylamide gel electrophoresis with 8 M urea. Ssl0564 was detected by its specific antibody. (B) Total RNA was isolated from cells exposed to various level of illumination for 15 min. 2 μg of total RNA per a lane was loaded for the detection of *rpe* and *ndhD2* transcripts and 6 μg was loaded for slr1957 transcript.

Fig. 10 Comparison of the effect of DCMU and DBMIB on the conformation of Ssl0564 and the expression level of its target genes, *rpe*, *ndhD2* and slr1957. (A) TCA fixed proteins from cells incubated under low-light conditions (LL), high-light conditions for 5 min (HL), HL conditions with 10 μM DCMU for 5 min (HL+DCMU) or HL conditions with 10 μM DBMIB for 5 min (HL+DBMIB) were alkylated and 7 μg of total protein per a lane was separated by non-reducing 15% SDS-polyacrylamide gel electrophoresis with 8 M urea. Ssl0564 was detected by its specific antibody. (B) Total RNA was isolated from cells incubated for 15 min under the same conditions used for (A). 2 μg of total RNA per a lane was loaded for the detection of *rpe* and *ndhD2* transcripts and 6 μg was loaded for slr1957 transcript.

Fig. 11 A schematic representation of photon flux density (PFD)-dependent transcriptional regulation achieved by PedR.

Table 1. List of ORFs whose expression level was affected by disruption of ssl0564.

ORF No.	Description	Induction by disruption of ssl0564 (fold)
slr1291	NAD(P)H dehydrogenase subunit 4 (*ndhD2*)	9.55 ± 5.50
ssl0564	transcriptional regulator	6.74 ± 1.76
sll0296	hypothetical protein	2.82 ± 0.51
sll0807	pentose-5-phosphate-3-epimerase (*rpe*)	2.65 ± 0.25
slr0749	protochlorophyllide reductase subunit ChlL (*chlL*)	0.22 ± 0.07
slr1957	hypothetical protein	0.25 ± 0.08
slr0750	protochlorophyllide reductase subunit ChlN (*chlN*)	0.33 ± 0.10
slr0772	protochlorophyllide reductase subunit ChlB (*chlB*)	0.34 ± 0.14

Values are averages ± standard deviation obtained from two independent and each duplicate results of DNA microarray experiments (n = 4).

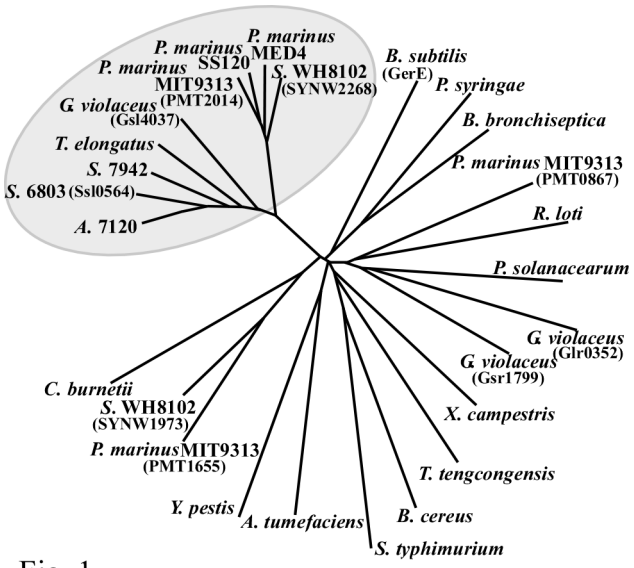
P. marinus MED4
P. marinus SS120
P. marinus MIT9313 (PMT2014)
S. WH8102 (SYNW2268)
G. violaceus (Gsl4037)
T. elongatus
S. 7942
S. 6803 (Ssl0564)
A. 7120
B. subtilis (GerE)
P. syringae
B. bronchiseptica
P. marinus MIT9313 (PMT0867)
R. loti
P. solanacearum
G. violaceus (Glr0352)
G. violaceus (Gsr1799)
X. campestris
T. tengcongensis
B. cereus
S. typhimurium
A. tumefaciens
Y. pestis
P. marinus MIT9313 (PMT1655)
S. WH8102 (SYNW1973)
C. burnetii

Fig. 1

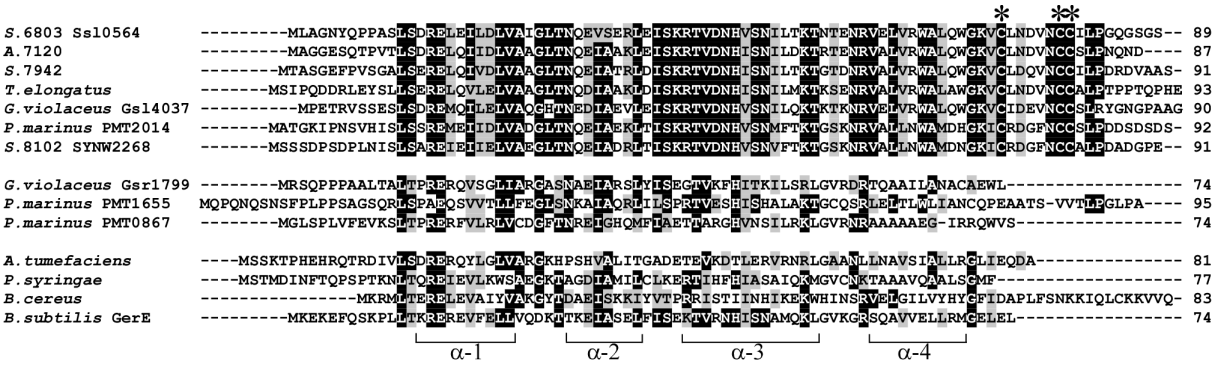
S.6803 Ssl0564 89
A.7120 87
S.7942 91
T.elongatus 93
G.violaceus Gsl4037 90
P.marinus PMT2014 92
S.8102 SYNW2268 91
G.violaceus Gsr1799 74
P.marinus PMT1655 95
P.marinus PMT0867 74
A.tumefaciens 81
P.syringae 77
B.cereus 83
B.subtilis GerE 74
α-1
α-2
α-3
α-4

Fig. 2

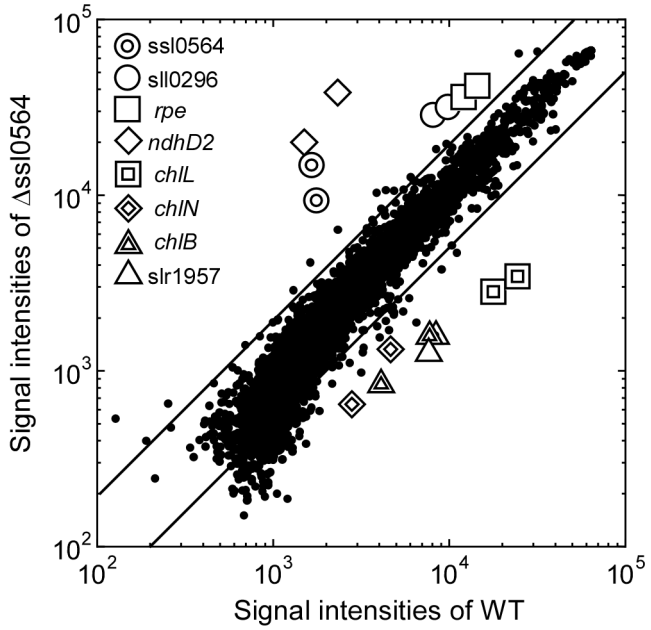
ssl0564
sll0296
rpe
ndhD2
chlL
chlN
chlB
slr1957
Signal intensities of Δssl0564
Signal intensities of WT
10^2
10^3
10^4
10^5

Fig. 3

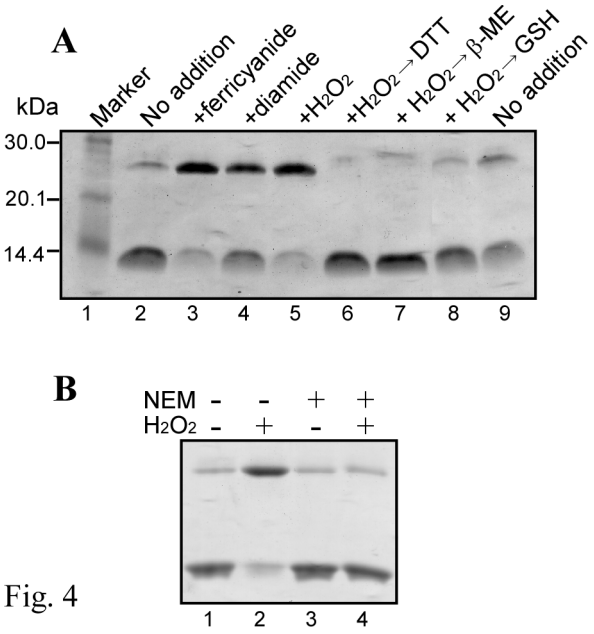
A
kDa
Marker
No addition
+ferricyanide
+diamide
+H2O2
+H2O2→DTT
+ H2O2→β-ME
+ H2O2→GSH
No addition
30.0
20.1
14.4
1 2 3 4 5 6 7 8 9
B
NEM - - + +
H2O2 - + - +
1 2 3 4

Fig. 4

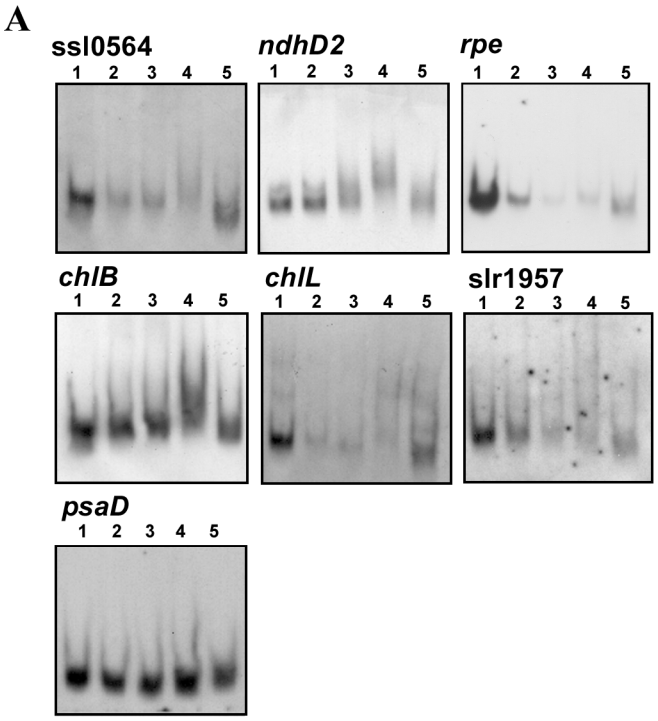
A
ssl0564
1 2 3 4 5
ndhD2
1 2 3 4 5
rpe
1 2 3 4 5
chlB
1 2 3 4 5
chlL
1 2 3 4 5
slr1957
1 2 3 4 5
psaD
1 2 3 4 5

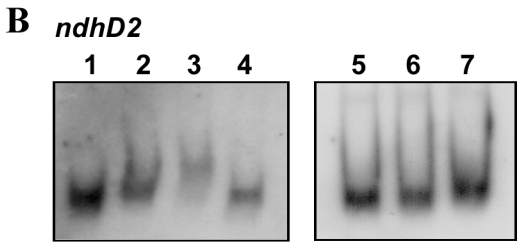
B
ndhD2
1 2 3 4
5 6 7

Fig. 5

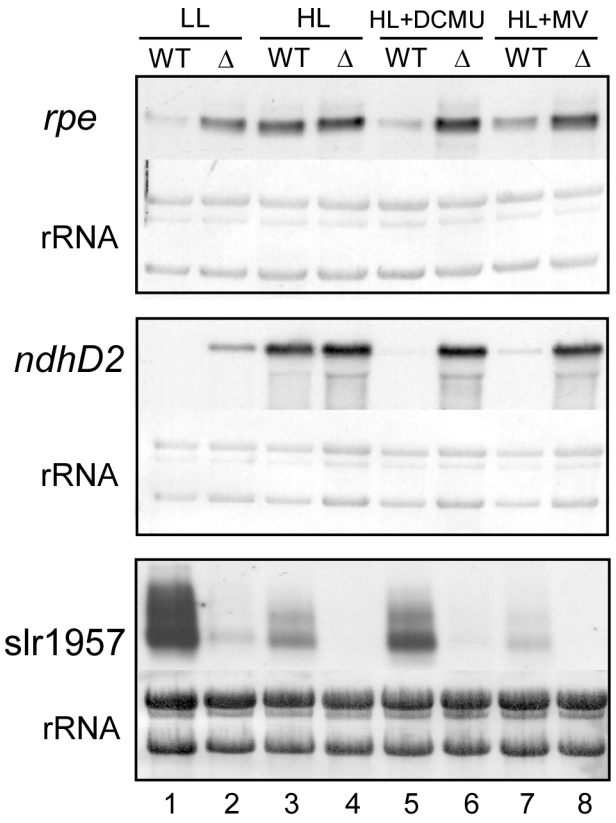
LL
HL
HL+DCMU
HL+MV
WT
Δ
WT
Δ
WT
Δ
WT
Δ
rpe
rRNA
ndhD2
rRNA
slr1957
rRNA
1
2
3
4
5
6
7
8

Fig. 6

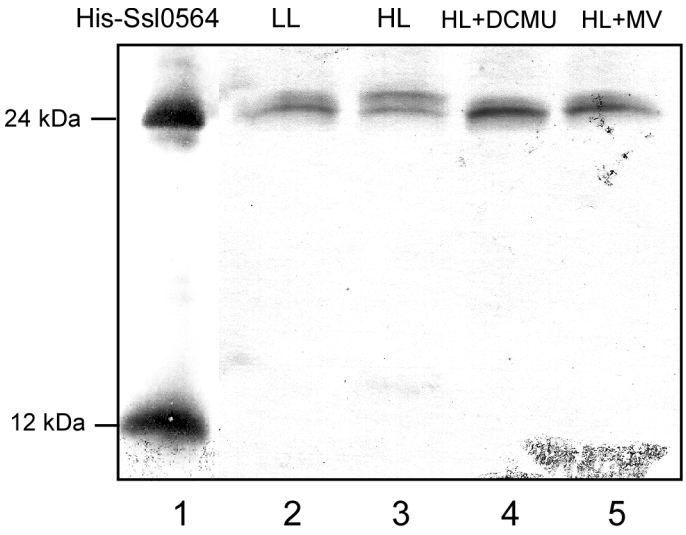

Fig. 7

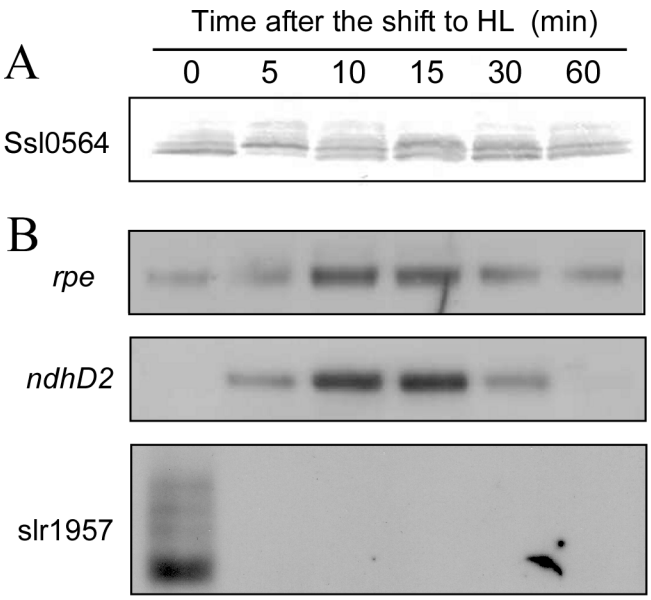
Time after the shift to HL (min)
A
0
5
10
15
30
60
Ssl0564
B
rpe
ndhD2
slr1957

Fig. 8

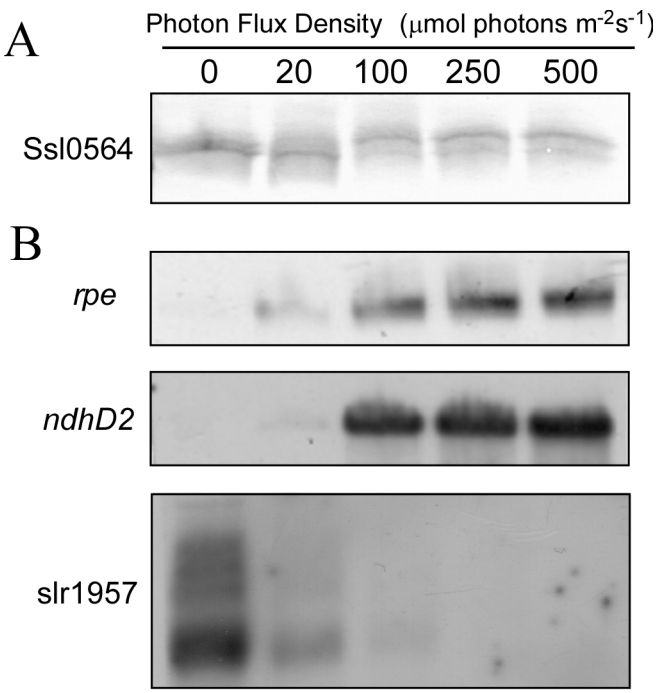
A
Photon Flux Density (μmol photons m-2s-1)
0
20
100
250
500
Ssl0564
B
rpe
ndhD2
slr1957

Fig. 9

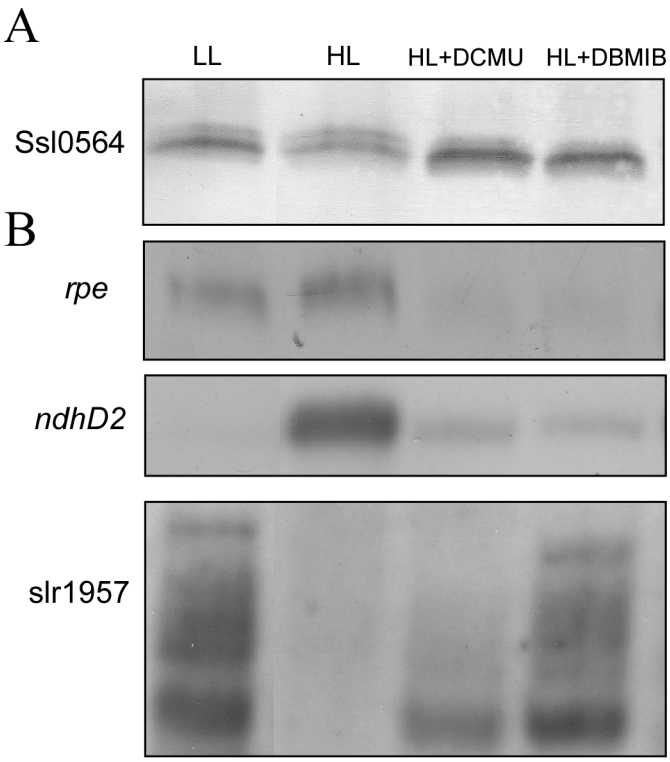

Fig. 10

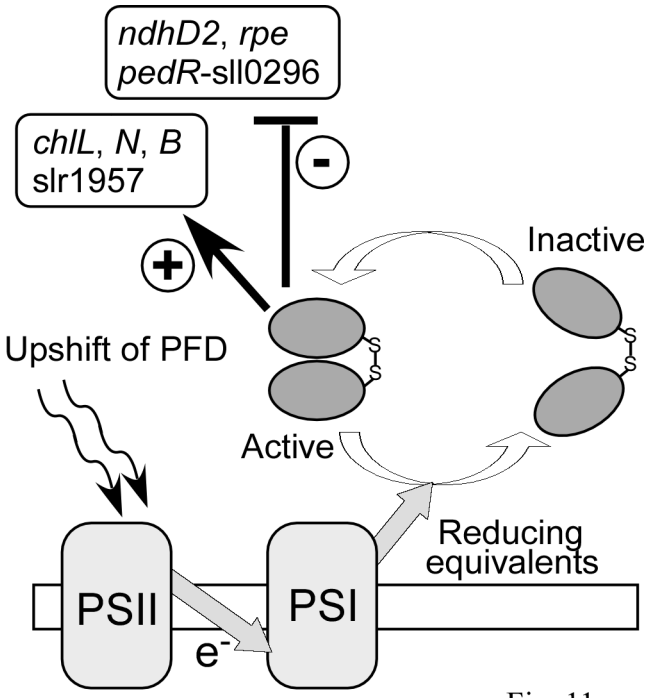
ndhD2, rpe
pedR-sll0296
chlL, N, B
slr1957
Inactive
Upshift of PFD
Active
Reducing
equivalents
PSII
PSI
e-

Fig. 11